

# X-Band Pulse-EPR Resonator Performance

Peter Höfer and Patrick Carl

EPR Division  
Bruker BioSpin GmbH  
76287 Rheinstetten, Germany

## Introduction

In the last decade, we have witnessed how Pulse-EPR has become a matured and well accepted analytical tool in science. With the ELEXSYS E 580 spectrometer, Bruker has pushed forward the field by a series of new developments. A considerable improvement in performance and handling has been achieved by digital electronics dedicated to EPR (SpecJet and PatternJet), microwave units (based on the intermediate frequency concept) for multi-frequency Pulse-EPR in X-, Q- and W-Band and accessories for the double-resonance techniques (Pulse-ENDOR and Pulse-ELDOR). Continuous efforts are necessary to keep up with the growing and changing demands. This is especially true for the probe-

heads which have been another major focus of development in the last years. One of the driving forces in resonator development was Double-Electron-Electron Resonance (DEER), a technique to determine the distance between two electron spins [1-3]. This technique requires a resonator with large bandwidth and high  $B_1$ , two conditions which are difficult to match simultaneously. In the following we present the recent improvements of our Flexline resonator series with respect to bandwidth and  $B_1$ , we investigate the relationship between size and signal-to-noise, and determine  $B_1$  homogeneity and background signals.

## Bandwidth and $B_1$

In standard pulse EPR, the required resonator bandwidth ( $\Delta\nu$ ) is determined by the shortest  $\pi/2$  pulse which can be generated with the given microwave power ( $P$ ). As a rule of thumb we have to fulfill the condition  $\Delta\nu \approx t_p(\pi/2)^{-1}$ . For a  $\pi/2$  pulse of 10 ns ( $B_1 = 25$  MHz) the resonator should then have a bandwidth of 100 MHz, corresponding to a quality factor  $Q = 100$  at an operating frequency of  $\nu = 10$  GHz.

As the microwave power is limited and

$$B_1 = c * (Q * P)^{1/2} \quad (1)$$

the resonator conversion factor,  $c$ , is the only parameter that can be increased to achieve high  $B_1$  at low  $Q$ . A means to increase  $c$  is to reduce the volume of the resonator. This approach has led to the development of various resonator structures: dielectric, split-ring, slotted tube and loop-gap [4-8]. Already with the ESP 380 Bruker had introduced the ER 4118X-MD-5 (dielectric) and the ER 4118X-MS-5 (split-ring) resonators, both with 5 mm sample access, to meet the above requirements. The demands on bandwidth and  $B_1$  have further increased with the popularity of DEER. In DEER two microwave frequencies are used, one to provide the detection pulses and the other one to supply the pump pulse. The separation of both frequencies can be up to 800 MHz in the Bruker ELDOR accessory E 580-400 and thus a corresponding resonator bandwidth is required. This demand has led to optimization of the coupling structures and to the new split-ring modules MS-3 and MS-2 with 3-mm and 2-mm sample access, respectively. The results of bandwidth and  $B_1$  measurements are compared in Fig. 1 for the MD-5 (top) and MS-2 (bottom). The measurements were performed with the standard 1 kW X-Band TWT amplifier. An electron spin  $S = 1/2$  sample (coal) was used in a nutation experiment to map out  $B_1$  in the rotating frame in 50 MHz steps across the frequency range of the X-Band pulse bridge. At maximum overcoupling a  $B_1$  of 25 MHz is achieved at

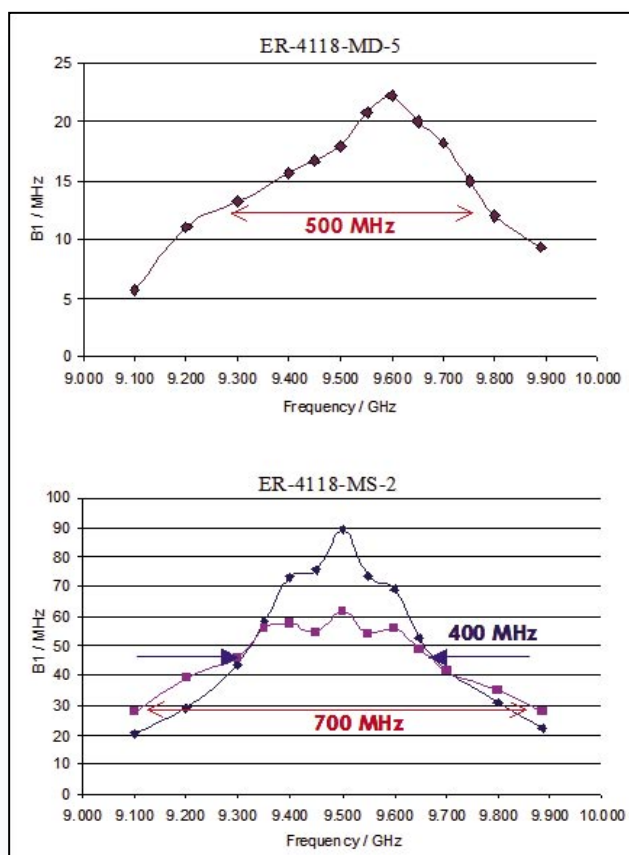


Fig. 1: EPR resonator bandwidth measured by e-nutation of  $S = 1/2$  system. Top = ER-4118-MD-5 and Bottom = ER4118-MS-2.

500 MHz bandwidth with the MD-5. The MS-2 shows at two different degrees of coupling a  $B_1$  of 90 and 60 MHz at 400 and 700 MHz bandwidth, respectively. For DEER experiments these are very comfortable numbers. In the case of distance determination between two spin labels the separation of the two microwave frequencies is around 50 - 70 MHz. With the much larger resonator bandwidth the experiment can be run without complicated pulse adjustment, a considerable improvement in ease of use. Furthermore, it provides additional experimental freedom in cases where samples other than spin labels are involved. **Table 1** shows the results obtained for all Flexline probes.

**Table 1**

	BW / MHz	Q	$B_1$ / MHz	$t (\pi/2)$ ns
MD-5	500	24	23	11
MS-5	240	40	37	6.75
MS-3	800	12	40	6.25
MS-2	400	24	90	2.80
	700	14	60	4

The combination of large bandwidth and high  $B_1$  is also beneficial in ELDOR detected NMR [9] in cases of large hyperfine interaction. This experiment involves a second microwave frequency driving forbidden EPR transition offset by the ENDOR (or NMR) frequency from the detection frequency. **Fig. 2** shows as an example the result obtained with the MD5 resonator from a sample containing  $Mn^{2+}$  (the inset in red shows the corresponding Davies-ENDOR spectrum). The total span of the spectrum is about 300 MHz, requiring a resonator bandwidth of that order and a  $B_1$  sufficiently high to drive the forbidden transitions. As the transition moment of the forbidden transitions is in general low and unknown, a high  $B_1$  is the key in experimental flexibility to set up the pump pulse.

Other important aspects of the resonator bandwidth are the related properties, signal-to-noise and dead-time ( $t_D$ ) for FID and echo detection. Their relation is given by

$$S/N \propto e^{-t_D/T_2} \cdot \sqrt{Q} \quad (2)$$

where  $T_2$  is the transverse electron spin relaxation time. Concerning  $S/N$  there are two competing effects, an increase with  $Q^{1/2}$  and a decrease resulting from the dead-time where  $t_D \propto Q$  holds. Thus there is an optimum  $Q$  for every  $T_2$  which is calculated as [10-11]

$$Q_{opt} = \pi * \nu * T_2 / 32 \quad (3)$$

In **Fig. 3** equation [2] is plotted for  $T_2$  of 100 ns and 1000 ns and shows that the optimum  $Q$  is about 100 and 1000, respectively.

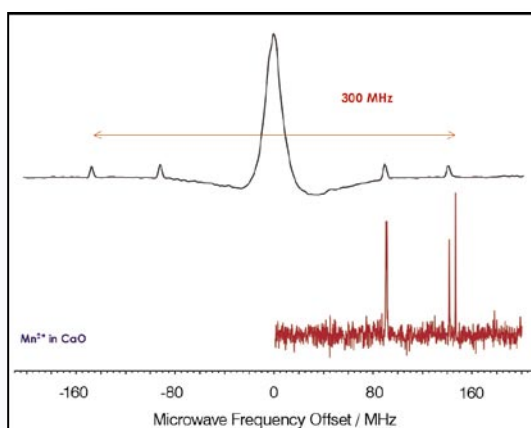


**Fig. 2:** ELDOR-Detected NMR spectrum (top) of  $Mn^{2+}$  in CaO and corresponding  $^{55}Mn$ -ENDOR spectrum

The strategy to optimize  $S/N$  by changing  $Q$  can be used in experiments where bandwidth is not of major concern, e.g. for Mims and Davies pulse-ENDOR spectra. As an example we show in **Fig. 4** the Davies ENDOR spectra of a powder sample of biphenyl in boric acid. A considerable gain in  $S/N$  could be achieved by changing  $Q$  to higher values than normally used. It should be noted that the sample  $T_2$  is  $5.3 \mu\text{sec}$  and the possible gain in  $S/N$  was not exhausted in this experiment.

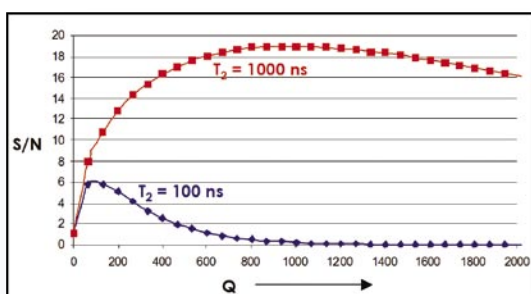


**Fig. 3:** Dependence of the signal to noise on resonator  $Q$ -value as calculated by equation 2 for  $T_2$  of 1000 ns and 100 ns.

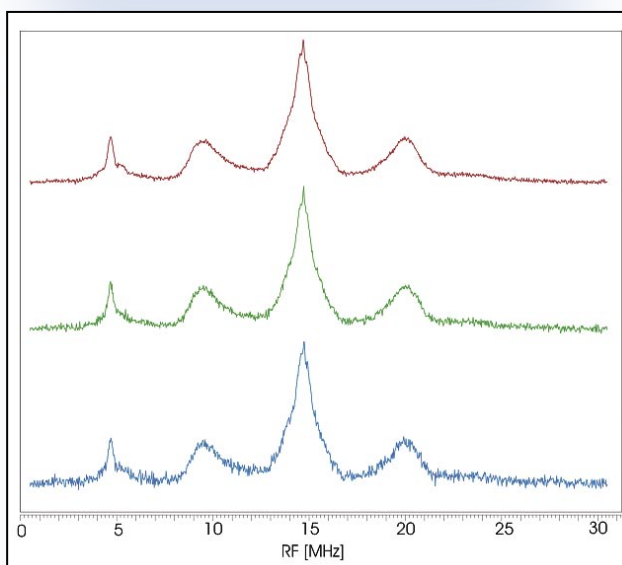


**Fig. 4:** Davies ENDOR spectra of biphenyl in boric acid powder ( $T_2 = 5.3 \mu\text{s}$ ) at various  $Q$ -values. **Top:**  $Q = 700$ , **Middle:**  $Q = 150$ , and **Bottom:**  $Q = 80$ .

## Signal-to-Noise and Resonator Volume

In the same way as the conversion factor is the handle to increase  $B_1$ , the conversion factor also enters in the detection sensitivity with  $S/N = c \times \sqrt{Q}$ . If we compare different resonators, the microwave power required for a given pulse then directly tells the relative sensitivity for a point sample. To compare volume samples we have to take into account the sample volume ( $V_S$ ) and the resonator volume ( $V_{Res}$ ) which enter into the  $S/N$  as [12]

$$S/N \propto V_S / V_{Res}^{1/2} \quad (4)$$

For the experimental comparison of the resonators, we used coal as a volume sample and a small DPPH crystal as a point sample. For the coal, a two pulse echo was applied with a pulse separation of 200 ns and pulse lengths of 16 ns. The coal sample was put in quartz tubes of suitable diameter with a filling height exceeding the resonator length. An FID generated by a 16 ns pulse was used for DPPH. For each resonator the  $Q$  was adjusted to 200, a value which can be determined and adjusted faithfully by means of the pulse ring-down time  $t_R$  with  $Q = \nu^* \pi^* t_R$ .

The resulting echo signals from the coal sample are shown in **Fig. 5** for the MD-5, MS-3 and MS-2 (top to bottom). As expected, the power required for maximum echo is decreasing with resonator size ( $P$  here denotes the attenuation

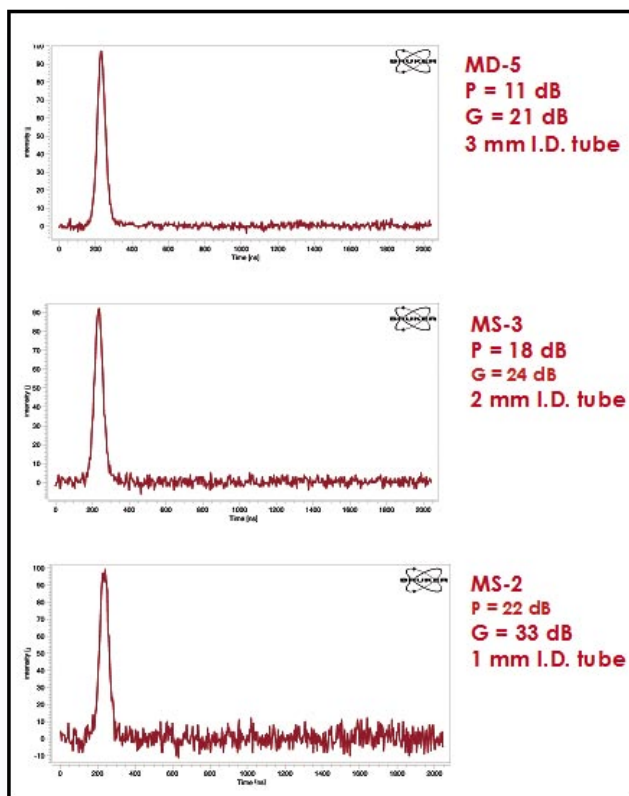


**Fig. 5:** Volume signal-to-noise for MD-5 (top), MS-3 (middle) and MS-2 (bottom) resonators.  $P$  denotes the attenuation of microwave pulse power and  $G$  denotes the receiver gain.

of the microwave pulse power). The gain in conversion factor can, however, not compensate the loss in sample volume and the echo  $S/N$  is decreasing with resonator size. On the other hand, in the case of a point sample the higher conversion factor is directly translated into a higher  $S/N$  for decreasing resonator size. The experimental and theoretical results for point and volume sample are compiled in **Table 2** for all Flexline probes. For easy comparison all results were normalized to the MD-5 which is also identical in performance to the Pulse-ENDOR version EN 4118X-MD-4. For the volume (line) samples an excellent agreement between theory and experiment was achieved. The relatively large deviation between theory and experiment for the point sample is most likely due to sample positioning errors. It is worthwhile to mention that the ESE- $S/N$  is one aspect to consider and the other one is the effect- $S/N$ , e.g. the ESEEM or DEER modulation depth. A larger modulation amplitude, generated by higher  $B_1$  and/or larger bandwidth, can indeed compensate a lower echo  $S/N$ .

**Table 2**

I.D. / L	$V_{Res}/\mu l$	Line sample		Point sample	
		$SN^{exp}$	$SN^{theory}$	$SN^{exp}$	$SN^{theory}$
MD-5/13	255	100%	100%	100%	100%
MS-5/6	117	77%	68%	100%	145%
MS-3/4	28	30%	33%	200%	300%
MS-2/6	19	22%	20%	340%	365%

Increasing signal-to-noise is also a major argument for higher operating frequencies of the EPR spectrometer. With our recently developed SuperQFT bridge and the new Q-band resonator ER 5107-D2 (13) we can make a direct comparison of the identical sample in X- and Q-band. Both resonators, the X-band MS-2 and the Q-Band ER 5107-D2 have the same inner diameter of 2 mm and accept the same sample tube. In this case the  $S/N$  scales as [12]

$$S/N \propto (\omega^3 * Q)^{1/2} \quad (5)$$

Taking into account the resonator lengths of 6 mm (MS-2) and 5 mm (D2) and the actual  $Q$  values of 24 in X-Band and 425 in Q-Band we expect an increase in  $S/N$  by a factor of 23 go-

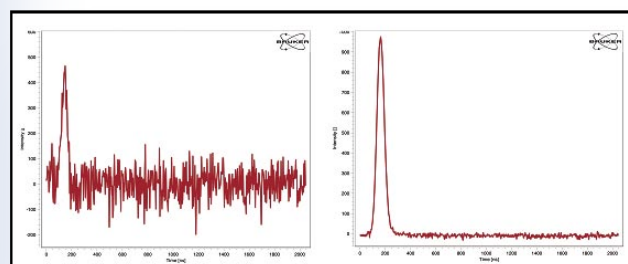


**Fig. 6:** Frequency dependence of volume signal-to-noise at X-band (left) with the ER-4118-MS-2 and at Q-band (right) with the ER

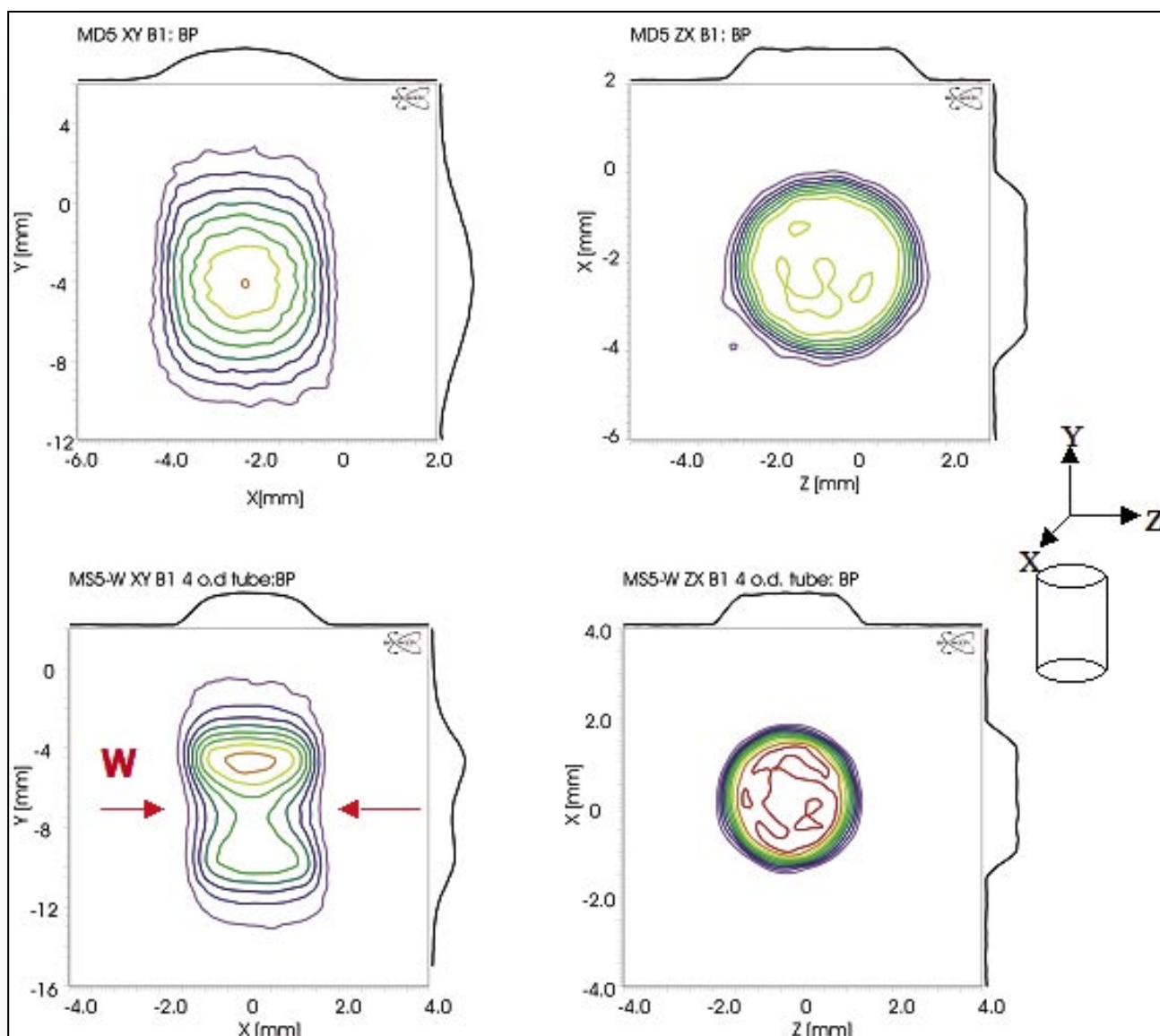


**Fig. 7:** 2D-Spatial EPR images of the ER-4118-MD-5 (top) and the ER-4118-MS-5W resonators. **Left:** EPR image of XY plane, projection across the diameter of the resonator. **Right:** EPR image of ZX plane, projection along the length of the resonator.

ing from X- to Q-Band. For experimental verification we have used a dilute coal sample in a 1 mm I.D. quartz tube (Z-pulse echo,  $\tau = 200$  ns, 9 shots averaged). The experimental gain in S/N by a factor of 20 (**Fig. 6**) is in good agreement with the expectation. In the course of the experiments it turned out that the signal from our standard coal sample is too large in Q-Band and we have therefore diluted the sample by a factor of 10.

### $B_1$ Homogeneity

Ideally one would desire a uniform  $B_1$  over the full resonator volume. In reality this is not the case and it is of importance for many experiments to be aware of the inhomogeneity of  $B_1$  across the sample. An elegant way to measure the  $B_1$  distribution is by means of a CW-EPR imaging experiment of a volume sample which preferably fills the entire resonator. For

low enough microwave power the CW-EPR signal amplitude is proportional to  $B_1$  and thus the spatial EPR image gives the  $B_1$  distribution over the volume of the sample. The CW-EPR signal amplitude also depends on the field modulation amplitude. As the modulation coils are much larger than the resonator the modulation field is assumed to be uniform over the sample volume. The imaging experiments were performed with a 1 mM solution of TEMPOL in toluene using the E 540 imaging accessory [14]. Planes showing the radial and axial  $B_1$  distribution were imaged with gradients of 40 G/cm. In **Fig. 7** we present the results obtained for the MD-5 with a 4-mm I.D. tube and for the MS-5W (W denoting the optical window) with a 3-mm I.D. tube. The image axis system is defined as Z parallel to  $B_0$ , Y parallel to the sample tube axis and X perpendicular to Z and Y.

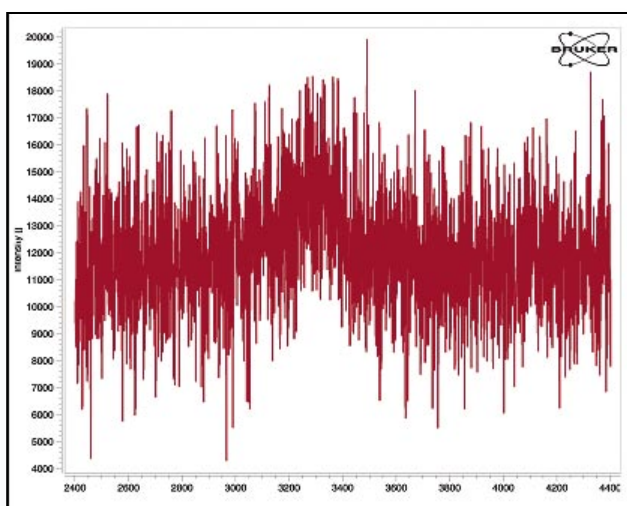


**Fig. 8:** Background signal at 5 K of an empty ER-4118-MS-2 resonator. Echo intensity was integrated 100 times at each field position.

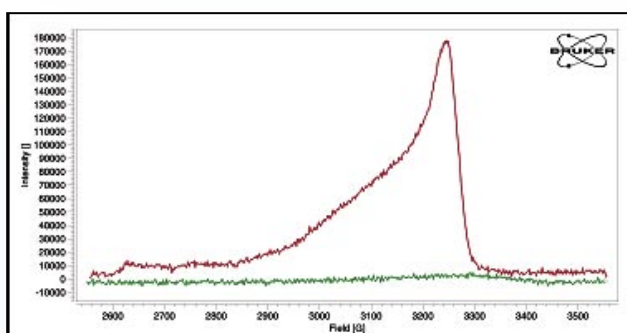


**Fig. 9:** Comparison of background signal from ER-4118-MS-2 resonator to 500  $\mu\text{M}$   $\text{CuSO}_4$  solution.

In the 2D imaging experiment, the signal intensity of the unresolved axis is integrated and projected onto the imaged plane, therefore the XY images show maximum intensity in the center along the Y axis (integral over the tube in Z direction). The skyline projections on the right of the XY images give the  $B_1$  distribution along the length of the resonator. The Y profile of the MD-5 (Fig. 7, top left) shows the expected bell shape while the MS-5W (Fig. 7, bottom left) clearly shows a dent due to the optical window in the front and back of the resonator body. A further asymmetry along Y is most probably due to the coupling structure, which is located at the lower end of the resonator. As the MD-5 is optically transparent there is no window in the resonator body itself but only in the outer shield. This window has almost no effect on the  $B_1$  distribution (not shown). For both resonators the radial distribution (Fig. 7, right) is very uniform.

## Background Signals

The higher the sensitivity of a resonator, the higher is its sensitivity for paramagnetic impurities in the resonator material and surrounding structure. A further complication arises when these small resonator are immersed in a cryostat for low temperature experiments and are cooled to the same temperature as the sample. As background signals can potentially limit the useful sensitivity of a resonator, we have undertaken extra efforts to eliminate paramagnetic impurities and set new benchmarks for the split ring resonators. For these tests we have used the standard ER 4118CF helium cryostat and cooled the empty resonator to 5 K. A two pulse echo with pulses of 16 ns, a pulse separation of 200 ns and 1 ms repetition time was used to measure the background signal over a 2 kG field range. **Fig. 8** shows the result obtained for the MS-2 resonator where the echo intensity was averaged 100 times at every field point. From this result, we calculate the single shot S/N of the background signal as less than 1/10! The pulse power was adjusted on an inserted calibration sample for maximum echo amplitude. Background signals from the vicinity of the resonator are more likely to show up at higher power than used for the sample in the resonator. With today's new design a test under the same conditions but with full microwave power does not result anymore in a change of the background signal (not shown). For a further quantification we compare the background signal to the signal from a 500  $\mu\text{M}$   $\text{CuSO}_4$  solution at 5 K, **Fig. 9**. Comparison of the integrated signal intensity over a 900 G field range reveals a background intensity corresponding to about  $15 \pm 5 \mu\text{M}$   $\text{Cu}^{2+}$  ions in solution.

## References

- [1] A. D. Milov, A. B. Ponomarev, Y. D. Tsvetkov, Chem. Phys. Lett. 110, 67 (1984).
- [2] R. G. Larsen, D. J. Singel, J. Chem. Phys. 98, 5134 (1993).
- [3] M. Pannier, S. Veit, A. Godt, G. Jeschke, H. W. Spiess, J. Magn. Reson. 142, 331, (2000).
- [4] R. Biehl, BRUKER Report 1/1986.
- [5] H. Brunner, K. H. Hausser and W. Veith, Europa Patent No. 86104886.6-2204
- [6] M. Mehring and F. Freysoldt, J. Phys. E13, 894 (1980).
- [7] W. Froncisz and J. S. Hyde, J. Magn. Reson. 47, 515 (1982).
- [8] S. Pfenninger, J. Forrer, A. Schweiger, and Th. Weiland, Rev. Sci. Instrum. 59, 752 (1988).
- [9] P. Schosseler, Th. Wacker, A. Schweiger, Chem. Phys. Lett. 224, 319 (1994).
- [10] J. Gorcester and J. H. Freed, J. Chem. Phys. 88, 4678 (1988).
- [11] P. Höfer, BRUKER Report 2/1989.
- [12] G. A. Rinard, R. W. Quine, J. R. Harbridge, R. Song, G. R. Eaton, S. S. Eaton, J. Magn. Reson. 140, 218 (1999).
- [13] P. Höfer, R. Heilig, D. C. Maier, I. Prisecaru, D. Schmalbein, BRUKER SpinReport 152/153.
- [14] EPR Division, BRUKER SpinReport 156.